# A small molecule inhibitor of RNA-binding protein IGF2BP3 shows anti-leukemic activity

Amit K. Jaiswal[1], Georgia M. Scherer[2*], Michelle L. Thaxton[1*], Jacob P. Sorrentino[2], Constance Yuen[3], Milauni M. Mehta[2], Gunjan Sharma[1], Tasha L. Lin[1], Tiffany M. Tran[1], Amanda Cohen[1], Alexander J. Ritter[4], Rishi S. Kotecha[5,6,7], Jeremy R. Sanford[4,8], Robert D. Damoiseaux[3,9,10,11] , Neil K. Garg[2] and Dinesh S. Rao[1,11,12]

*[1] Department of Pathology and Laboratory Medicine, University of California, Los Angeles, CA, USA*
*[2]Department of Chemistry and Biochemistry, University of California, Los Angeles, CA, USA*
*[3]California Nanosystems Institute, University of California, Los Angeles, CA, 90095, USA*
*[4] Department of Molecular, Cell and Developmental Biology and Center for Molecular Biology of RNA, University of California, Santa Cruz, CA, USA*
*[5]Department of Clinical Haematology, Oncology, Blood and Marrow Transplantation, Perth Childrens Hospital, Perth, Australia*
*[6]Leukemia Translational Research Laboratory, WA Kids Cancer Centre, University of Western Australia, Perth Australia*
*[7]Curtin Medical School, Curtin University, Perth, Australia*
*[8]Center for Biomolecular Science & Engineering, University of California, Santa Cruz, CA*
*[9]Department of Molecular and Medical Pharmacology, University of California, Los Angeles, CA, USA*
*[10]Department of Bioengineering, Samueli School of Engineering, University of California, Los Angeles, CA, 90095, USA*
*[11]Jonsson Comprehensive Cancer Center, University of California Los Angeles, CA, USA*
*[12]Broad Stem Cell Research Center, University of California Los Angeles, CA, USA*

*These authors contributed equally to this manuscript.

**Corresponding Author:**
Dinesh S. Rao, M.D., Ph.D.,
Professor
Department of Pathology and Laboratory Medicine
David Geffen School of Medicine at UCLA
650 Charles E Young Drive, 12-272 Factor
Los Angeles, CA 90095
Tel. 310-825-1675
Fax. 310-825-0814
Email drao@mednet.ucla.edu

**ABSTRACT**

The RNA-binding protein IGF2BP3 is an oncofetal protein overexpressed in B-acute lymphoblastic leukemia and is critical for leukemogenesis in experimental models. With cancer-specific expression, functional dispensability for normal development, and an unleveraged pro-oncogenic function in mRNA homeostasis, IGF2BP3 represents an excellent target. With no small molecule inhibitors of IGF2BP3 in clinical use, we undertook an effort to identify new IGF2BP3 inhibitors using biochemical methods. A biochemical screen, followed by a cell-based counter screen, led to the identification of compounds with protein-RNA interaction inhibition and leukemic cell growth-inhibitory activity. One of these compounds, designated I3IN-002, shows consistent cell growth-inhibitory activity, altered cell cycle and increased apoptosis in multiple leukemia cell lines, and is the most potent inhibitor of IGF2BP3 reported to date. I3IN-002 was tolerated in mice when administered intraperitoneally and showed potent anti-leukemic activity in a syngeneic transplantation model of MLL-Af4 leukemia. I3IN-002 inhibits the function of IGF2BP3, disrupting in situ binding of IGF2BP3 to target mRNAs, and altering IGF2BP3-dependent gene expression regulation. Furthermore, cell-free and cellular thermal shift assays as well as drug affinity responsive target stability assays support on target activity of I3IN-002 for IGF2BP3. Thus, the identification of I3IN-002 paves the way for the discovery of potent and selective small molecule inhibitors of IGF2BP3.

69 **SIGNIFICANCE**

70 In this manuscript, we have identified a small drug like molecule, I3IN-002, which shows anti-
71 leukemic activity, disrupts IGF2BP3 function in leukemia cells, and paves the for future translation
72 to the clinic.

73 **INTRODUCTION**

74 RNA binding proteins (RBPs) are important players in post-transcriptional gene regulation,
75 defined as regulation that occurs following the production of an mRNA transcript. Many RBPs are
76 thought to play a house-keeping role in gene regulation, but others show cancer-specific
77 expression and may regulate oncogenesis via diverse mechanisms [1-5]. The RNA binding
78 protein IGF2BP3 was initially discovered as a factor overexpressed in pancreatic cancer and one
79 of three homologous proteins (IGF2BP1-3) that bound to the 5'-untranslated region of the IGF2
80 mRNA (1,2). Since its original description, a large body of work has congruently demonstrated
81 its role as an oncogenic protein in a number of different cancers, and that IGF2BP3 binds to the
82 3'UTR of mRNA (3). In acute leukemia, we and others initially identified IGF2BP3 as an
83 upregulated RBP in MLL-translocated B-ALL (4,5). IGF2BP3 is transcriptionally induced by MLL-
84 AF4, and its expression seems to be restricted to this subtype of acute leukemia. In vivo,
85 overexpression of IGF2BP3 in bone marrow led to hyperproliferation in hematopoietic stem and
86 progenitor cells and a pre-leukemic disease with expansion of B- and myeloid cells (4). Moreover,
87 deletion of *Igf2bp3* in vivo significantly limited leukemia development and increased leukemia-
88 free survival (6,7). At baseline, the *Igf2bp3* knockout mouse did not show any overt phenotypes,
89 suggesting that it is dispensable for normal development and homeostasis in the adult. Together
90 these studies establish IGF2BP3 as an oncogenic target in acute leukemia.

91

92 To investigate the molecular mechanisms of IGF2BP3's action, we previously undertook iCLIP-
93 seq, a technique designed to globally detect RNA molecules bound by IGF2BP3 in conjunction
94 with differential expression analyses in cells that were depleted for IGF2BP3. These analyses
95 revealed that IGF2BP3 most commonly binds to the 3'UTR of mRNA transcripts. The regulated
96 mRNA transcripts included numerous downregulated oncogenes such as *HOXA9*, *CDK6* and
97 *MYC* (4,6). Importantly, deletion of the RNA-binding domains of IGF2BP3 abrogated stabilization

98 of these transcripts, and reversed IGF2BP3-driven pre-leukemic disease in vivo (4). Together
99 these data suggest that IGF2BP3's binding to specific mRNAs is central to its role in promoting
100 oncogenesis in the hematopoietic system. In addition, data generated by others has now revealed
101 that epitranscriptomic modification of target mRNAs with N6-methyladenosine ($m^6A$) is a
102 determinant of IGF2BP3 binding and function, and that spacing between short stretches of RNA
103 also play a role (8-11). These specific determinants of mRNA binding (i.e., sequence, spacing,
104 $m^6A$ modifications) by IGF2BP3 formed the basis of our mechanistic understanding of the activity
105 of this protein. Interference with IGF2BP3 RNA-binding function phenocopies IGF2BP3 loss-of-
106 function, based on our prior studies (4,6).
107
108 RBPs were previously under-represented in targeted therapy approaches due to their presumed
109 "undruggable" status, recent efforts have uncovered a number of small molecules targeting RBPs,
110 including the IGF2BP family (12,13). With the oncogenic role of IGF2BP3 established by not only
111 our studies but also hundreds of studies in the literature, we sought to identify a small molecule
112 inhibitor of the protein. This would not only serve as a tool compound for further understanding
113 the mechanism of IGF2BP3, but also as a starting point for a potential therapeutic. To this end,
114 we developed and validated a time-resolved Förster resonance energy transfer (TR-FRET) assay,
115 using purified IGF2BP3 protein and a synthetic $m^6A$-modified target RNA molecule to measure
116 binding. A library of small molecule compounds was applied to this assay, with resultant hit
117 compounds being re-confirmed in TR-FRET assays and counter screened in cell-based assays.
118 Confirmatory studies to demonstrate activity in several leukemia cell lines with IGF2BP3
119 overexpression showed inhibition of cell growth and cell cycle progression, and increased
120 apoptosis. The first of these compounds, referred to here as I3IN-002, shows activity against
121 leukemic initiating cells in vitro, and has anti-leukemic activity in vivo. I3IN-002 directly interferes
122 with the function of IGF2BP3, as assessed by gene expression analyses and RNA

123 immunoprecipitation experiments that measure IGF2BP3-dependent gene expression and
124 IGF2BP3-mRNA binding. Furthermore, cellular thermal shift assays, cell-free thermal shift assay
125 (TSA), drug affinity responsive target stability (DARTS) support on-target activity for I3IN-002.
126 I3IN-002 may prove useful as a tool compound in future biochemical studies involving IGF2BP3
127 and may also enable the development of a novel therapeutics for the treatment of leukemia and
128 other cancer types.

129 **RESULTS**

130 **Disruptors of protein-RNA interactions are identified via biochemical screening.** Despite
131 the extensive literature describing the cancer-specific function of IGF2BP3, small molecules that
132 specifically target this protein have not yet made any forays into the clinic, and have not been
133 extensively described as tool compounds to explore function. More specifically, a couple of small
134 molecules [32] have been shown to decrease expression of IGF2BP3, and only one compound
135 has been reported to directly inhibit IGF2BP3, with $IC_{50}$ values of 10–40 μM across various ovarian
136 cancer cell lines [35]. To identify putative inhibitors of IGF2BP3 (I3), we designed and validated a
137 time-resolved Förster resonance energy transfer (TR-FRET) assay, based on binding of a GFP-
138 tagged I3 (I3-GFP) to a biotinylated RNA oligonucleotide carrying a $m^6A$ modification (**Fig. 1a**).
139 Small molecules that interfere with this interaction will lead to a loss of signal transfer, and
140 subsequently decreased GFP fluorescence. For this assay, we generated a GFP- and FLAG-
141 tagged IGF2BP3 protein-encoding mammalian expression vector, by adding GFP- and FLAG tags
142 to the carboxy-terminus of the protein (3' end of the DNA construct) and cloned into pcDNA3.1
143 (**Supp. Fig. 1a**). We confirmed a functional fusion protein based on bright fluorescence following
144 transfection and recognition with anti-IGF2BP3 antibodies (**Supp. Fig. 1b**). The protein was
145 purified by elutions from fractions 3-11 on an anti-FLAG column (**Supp. Fig. 1c**) and subsequently
146 concentrated and quantitated by Coomassie staining (**Supp. Fig. 1d**). Functionality of the protein
147 was further confirmed by RNA immunoprecipitation of target mRNAs such as CDK6 and MYC
148 following incubation of purified protein and pulldown with anti-Flag (**Supp. Fig. 1e-g**). Following
149 purification and confirmation of RNA-binding activity, we confirmed that GFP fluorescence in the
150 TR-FRET assay required the presence of all components (i.e., I3-GFP, biotinylated mRNA, and
151 Terbium, **Fig. 1b**). Protein and RNA concentration dependence of the assay was demonstrated
152 with saturation of the GFP fluorescence signal at approximately 50 nM of I3-GFP-F and 25 nM
153 RNA oligonucleotide **(Fig. 1c and Supp. Fig. 1h)**. Next, we evaluated assay reproducibility across

154 multiple experiments performed across multiple days, finding excellent concordance in GFP
155 fluorescence and Z'-values (**Supp. Fig. 1i-j**).
156
157 To adapt the assay to high throughput screening, we first successfully miniaturized the assay to
158 10 μL, while maintaining σ+ <20% and Z'>0.5, with highly reproducible GFP fluorescence (**Supp.**
159 **Fig. 1k**). Following this validation, a high throughput screen of 196,567 compounds was
160 completed in two stages, a preliminary screen, and a full-scale screen. We were able to
161 successfully complete the screen: across 617 plates that were analyzed for this assay, we
162 achieved >99% of plates that showed standard deviation <20% and 95% of plates showed a Z'
163 score greater than 0.5 (**Supp. Fig. 2c** and **Fig. 1d**). Plates that showed a low Z'-score were
164 excluded from downstream hit confirmation. To define hits, we leveraged the preliminary screen
165 to increase the specificity of hit definition (**Supp. Fig. 2 a-c**). Using only the primary criterion,
166 defined as |Ratio Z|>3 (where Ratio is the ratio of terbium fluorescence/GFP fluorescence),
167 corresponding to a greater than 3-standard deviation change in fluorescence from controls, we
168 obtained a hit rate of 1.33% in the preliminary screen, and 1.73% in the full-scale screen (**Fig.**
169 **1e**). Using a secondary criterion, where Terbium fluorescence ("W1") was within one standard
170 deviation of the mean for the plate (i.e., |W1 Z|<1), this reduced the hit rate to 0.94% and 0.19%
171 in preliminary and full-scale screens respectively (**Fig. 1e**). The reduced hit rate in the full-scale
172 screen therefore is most likely due to increased variability in terbium fluorescence. Further
173 refinements of hits, by an alternate secondary criterion definition (mean and standard deviation
174 calculated for the experimental run, rather than the plate) and manual curation of the data when
175 irregularities were observed, led to an initial, high-stringency list of 417 compounds that were
176 further analyzed. Of the 417 hits out of 186,978 evaluable compounds, 29 contained a core
177 structure with an indolyltriazine group (**Fig. 1f**). Remarkably, the library only contained 174 total
178 compounds with the general structure depicted in **Fig. 1f**, representing ~74-fold enrichment

179 (range of 57-87-fold, depending on manual curation) for these compounds, a highly statistically
180 significant result (**Fig. 1g;** p<0.0001; Fisher's exact test). Together, our results identify a number
181 of small molecules with in vitro activity against the RNA binding activity of IGF2BP3.
182
183 **Cell-based counter screen identifies molecules with anti-leukemic activity.**
184 To further characterize the hits identified from the screen, we first performed a confirmatory TR-
185 FRET assay, with two experiments consisting of three replicates each. Concordant TR-FRET
186 findings were characterized as Tier 1, 2 and 3, when findings were reproduced in 2/2, 1/2, or 0/2
187 experiments respectively. 89.3% (371/417) of hit compounds and 93.1% (27/29) of indolyltriazine
188 compounds were Tier 1 or Tier 2 hits, respectively (**Supp. Fig. 2d**). Of note, mapping these
189 compounds back to the primary data from the full-scale screen did not show any obvious trends
190 in terms of the original single measured parameters in terms of compounds that were Tier 1, Tier
191 2, or Tier 3 (non-hits). To further examine these confirmed hits, we turned to a cell-based assay
192 (**Fig. 2a**). Here, we reasoned that a compound that was specific for IGF2BP3 would only show
193 activity in SEM cell lines that contained intact, increased expression of the protein (SEM-WT),
194 and should show reduced activity in cell lines where we had experimentally deleted the protein
195 via CRISPR-Cas9 (SEM-I3KO) (14). Cells were treated with compound, grown for 4 days under
196 normal growth conditions, and assayed for cell growth with CellTiter-Glo, a luminescence-based
197 reagent described previously (6,14,15). Fold change from control (i.e., no compound treated
198 wells) was plotted for SEM-WT versus SEM-I3KO. Remarkably, there were many compounds
199 that showed enhanced reduction of cell growth in SEM-WT, as opposed to SEM-I3KO (**Fig. 2b**).
200 We also wanted to include compounds with a significant effect on growth in WTs, even if the
201 change in the cellular growth ratio was more marginal. Using the cutoff (Growth Ratio<0.7 OR
202 WT Growth<0.7), we identified 16 compounds. We then chose three promising compounds,
203 designated **1**, **2** and **3** here, and tested them across a range of concentrations on SEM cells (**Fig.**

204 **2c-e**). Of these, **2** and **3**, which we later designated as **I3IN-002** and **I3IN-003**, showed differential
205 activity in the two cell lines, with **2** showing a promising $IC_{50}$ of ~2 μM in wild-type SEM-cells (**Fig.**
206 **2d**).
207
208 **I3IN-002 inhibits cell proliferation and cell cycle progression and promotes apoptosis.**
209 To enable further biological evaluation, we sought to prepare **I3IN-002** in high purity and in larger
210 quantities compared to what was available commercially. Moreover, chemical characterization
211 data for **I3IN-002** was not identified in the literature. To access **I3IN-002**, we performed the
212 synthetic route shown in (**Fig. 3a**). First isatin **4** was treated with thiosemicarbazide (**5**) and
213 potassium carbonate in methanol at ambient temperature to give hydrazone formation. The
214 hydrazone intermediate was subjected to potassium carbonate in water at reflux to give
215 triazinoindolothione **6** (16). In the next step, intermediate **6** was treated with alkyl chloride **7** in the
216 presence of potassium carbonate in DMSO (17). This delivered **I3IN-002**, which was isolated as
217 a powder. The purity of **I3IN-002** was deemed to be >97% by both quantitative $^{1}H$ NMR and HPLC
218 analysis.
219
220 To characterize the activity of I3IN-002, we tested the compound in a number of leukemia models,
221 including SEM, RS4;11, PER 785, KASUMI-2, NALM6, REH, and MLL-Af4 Lin- cells. The IC50
222 experiments performed on these cell lines showed the compound is more potent in B-ALL cell
223 lines with MLL-AF4 translocation, with lower IC50 values compared to other B-ALL cells (**Fig. 3b**).
224 Remarkably, treatment with a single dose of I3IN-002 resulted in a dose-dependent growth
225 inhibition of SEM, RS4;11 and Lin-MLL-Af4 cells at the concentrations tested in our assays (**Fig.**
226 **3c-e**). Moreover, cell cycle profiling using propidium iodide in SEM and RS4;11 cells both showed
227 an increase in sub-G0 cells (**Fig. 3f and Supp. Fig. 3a-3c**); changes in other phases of cell cycle
228 were not as consistent, because in SEM cells the G2-M transition genes such as CDK1 and

229 CCNB2, which are also IGF2BP3 targets, were downregulated due to compound treatment
230 (**Supp. Fig. 3d-3e**). Next, we analyzed the effect of I3IN-002 on cellular apoptosis. These studies
231 suggest an increase in apoptosis, as detected by Caspase 3/7 activity in both SEM and RS4;11
232 cells (**Fig. 3g and Supp. Fig. 3f**, respectively). Treatment also led to a numerically small but
233 statistically significant increase in Annexin V+ cells as well as in necrotic cells (Annexin V+ and
234 Propidium iodide+) in both SEM and RS4;11 cells (**Fig. 3h and Supp. Fig. 3g-i**). Together, these
235 studies indicate that I3IN-002 impacts cell growth, cell cycle and apoptosis in a variety of target
236 cell lines, including four different models of MLL-AF4-driven leukemia, and one AML cell line.
237 Moreover, the effect is conserved between species, in both human and murine cell lines.
238
239 **Reduction of leukemia initiating cells and leukemia engraftment in vivo by I3IN-002.**
240 Given our previous work showing that genetic ablation of *Igf2bp3* led to a reduction in leukemia
241 initiating cells, we next assayed whether I3IN-002 caused an effect on plating efficiency in
242 methylcellulose colony formation assays. Like I3KO, I3IN-002 led to a reduction in total colony
243 counts in a dose-dependent manner and a reduction in the fraction of cells that showed
244 expression of CD34 and c-kit (**Fig. 3i-j and Supp. Fig. 3j**). With these findings, we next evaluated
245 the compounds in vivo.
246
247 Next, mice syngeneically transplanted with the Lin-MLL-Af4 cells (either WT or I3KO, **Supp. Fig.**
248 **4a**) were injected intraperitoneally with I3IN-002 or vehicle control using the schedule indicated
249 (**Fig. 4a**). This model demonstrates a rapid and lethal leukemia that primarily involves the bone
250 marrow and spleen, with lesser involvement of the peripheral blood. Importantly, genetic ablation
251 of *Igf2bp3* extends survival and prevents leukemia development for greater than 100 days (14,15).
252 Here, we used the genetic deletion as a positive control for the predicted effect of IGF2BP3
253 inhibition. Upon harvest at 4 weeks post-transplant, WT-transplanted mice that received I3IN-002

254 showed significantly reduced spleen size and weight compared to vehicle treated control mice,
255 but larger than I3KO-transplanted mice (**Fig. 4b and 4d**). Histologically, we observed lower levels
256 of leukemic engraftment in the liver (compare cellular area next to arrow) and reduced
257 architectural distortion and lower leukemic engraftment in the spleen (compare size of dotted
258 areas and intervening cellularity) in I3IN-002 treated mice, and as expected in I3KO (**Fig. 4c**).
259 Similar reductions in engraftment were also noted in lung and kidney (**Supp. Fig. 4f**). Similar to
260 what was observed in vitro, FACS analysis revealed that in vivo treatment reduced the number of
261 CD34+ c-kit+ cells in both the spleen and the bone marrow (**Fig. 4e (spleen), 4h and 4k**). In the
262 spleen, leukemic engraftment and the proportion of CD11b+ cells and of CD34+ Sca1- cells were
263 reduced significantly (**Fig. 4f-g** and **Supp. Fig. 4b-4c**). In the bone marrow, overall leukemic
264 engraftment was not different following I3IN-002 treatment compared to vehicle, but significant
265 reductions in CD11b+ and CD34+ Sca1- cells were noted (**Fig. 4j** and **Supp. 4d-4e**). Further, we
266 found significant improvement in overall survival following I3IN-002 treatment in a separate set of
267 endpoint experiments (**Fig. 4l**). Together, these data indicate a significant effect by intraperitoneal
268 injection of I3IN-002 on leukemic burden, as measured by gross microscopic histology and flow
269 cytometry, and corresponding with a reduction in the leukemic initiating cell fraction, thus inhibiting
270 leukemogenesis and extending survival.
271
272 **I3IN-002 inhibits the molecular function of IGF2BP3 in post-transcriptional gene regulation.**
273 Prior work by our group and others (18) has shown that IGF2BP3 functions in post-transcriptional
274 gene regulation by binding to mRNA molecules and regulating their expression. To test whether
275 I3IN-002, a compound discovered via biochemical screening and confirmed to have cellular
276 activity, acts through IGF2BP3, we first performed RNA immunoprecipitation (RIP) following
277 treatment with I3IN-002. We found that four mRNAs that we have previously found to be
278 associated with IGF2BP3, *CDK6, MYC, BCL2,* and *HOXA9*, were decreased in the

279 immunoprecipitate following IGF2BP3 pulldown (**Fig. 5a-b** and **Supp. Fig. 5a-b**). Next, to assess
280 *in situ* binding of I3IN-002 to IGF2BP3, we performed a cellular thermal shift assay, finding a
281 difference in thermal stability, as assessed by Western blot **(Fig. 5c-d**). Direct interaction of I3IN-
282 002 with IGF2BP3 was confirmed using orthogonal methods. Thermal shift assay (TSA) using
283 purified full length IGF2BP3 demonstrated stabilization of IGF2BP3 with compound (**Fig. 5e**),
284 while DARTS demonstrated I3IN-002 dependent inhibition of protease mediated degradation of
285 IGF2BP3 (**Supp. Fig. 5c**). To understand the downstream consequences of IGF2BP3 inhibition,
286 we performed RNA-seq of DMSO-treated, I3IN-002-treated and I3KO SEM cells. These studies
287 resulted in the identification of differentially expressed genes between SEM-WT and SEM-I3KO
288 (n=319 genes) as well as between SEM-WT and SEM-WT-I3IN-002 treated cells (n=226 genes).
289 Volcano plots demonstrated that the overall changes in gene expression were more pronounced
290 in the genetic knockout of IGF2BP3 compared to I3IN-002 treated cells (**Fig. 5f**). However, the
291 relative proportion of downregulated and upregulated genes appeared to be somewhat similar.
292 Remarkably, 63 genes were common between the two datasets, which represents a highly
293 significant overlap (nearly 28% of genes regulated by I3IN-002 treatment; Hypergeometric test,
294 p-value< $10^{-16}$; **Fig. 5g**). Gene set enrichment analyses of the overlap genes between I3KO and
295 I3IN-002 treated cells showed many pathways that we have previously associated with IGF2BP3
296 function, including response to oxidative stress, cell activation, cellular response to cytokine
297 stimulus, neutrophil degranulation, etc. (**Fig. 5h**). A selected panel of differentially regulated
298 genes were confirmed by RT-qPCR (**Fig. 5i-n and Supp. Fig. 5e-f**), and Western blotting
299 confirmed the downregulation of CDK6 and BCL2 proteins that we have previously observed with
300 I3KO (**Fig. 5o**). Given these findings, we also queried the expression of various IGF2BP3 targeted
301 mRNAs in spleen specimens from mice treated in vivo, as described in **Fig. 4**. Several mRNAs,
302 including Myc, Cdk6, and Hoxa9 were downregulated in spleen samples from mice treated with
303 I3IN-002 based on RT-qPCR (**Supp. Fig. 5g-5l**). While these findings support a mechanism

304 wherein I3IN-002 is binding to and impacting the function of IGF2BP3, off-target effects cannot

305 be ruled out.

306 **DISCUSSION**

307 The RNA-binding protein IGF2BP3 is a potent oncofetal protein, as demonstrated by our work
308 and that of many others. We chose IGF2BP3 as a target in acute leukemia following our work
309 demonstrating that it is overexpressed in patients with MLL-AF4 translocated acute leukemia,
310 from genetic gain and loss-of-function experiments in cell lines and mouse models, and a
311 mechanistic understanding of its RNA binding function. In this manuscript, we describe the
312 successful completion of a high-throughput biochemical screening assay that utilizes the RNA-
313 binding function of IGF2BP3 as the discriminant for small molecule activity. Combining the
314 biochemical screen with a cell-based assay to detect IGF2BP3-dependent effects on leukemic
315 cell growth and survival, we identified 16 compounds that are likely to have activity in an IGF2BP3-
316 specific manner. The first of these compounds to be confirmed is I3IN-002, which shows an $IC_{50}$
317 of approximately 2 μM in initial assays. Specifically, I3IN-002 inhibited cell growth, impacted cell
318 cycle progression of treated cells, and increased apoptosis. I3IN-002 inhibited leukemia initiating
319 cells and showed in vivo anti-leukemic activity. Furthermore, I3IN-002 impacted global gene
320 expression in a manner similar to genetic deletion of IGF2BP3. CETSA, TSA, DARTS and RNA
321 immunoprecipitation experiments supported on-target activity against IGF2BP3. These results
322 provide evidence that I3IN-002 inhibits IGF2BP3.

323

324 RNA binding proteins have recently been appreciated as biologically and clinically significant
325 regulators of gene expression (12,19-21). This recognition has led to a growing effort to target
326 RNA binding proteins with small molecule or oligonucleotide-based strategies (12,22). However,
327 many cancer-associated RNA binding proteins are also required for normal homeostasis, and
328 hence, targeting these proteins might engender significant toxicity. Given this concern, discerning
329 RBPs that have cancer-specific expression is a major effort in the field, and the IGF2BP family of
330 proteins have emerged as cancer-specific or cancer-enriched proteins. Second, while

331 oligonucleotide-based therapies hold great promise, targeting of many tissues, including cancer,
332 remains a major challenge in the field. Hence, small molecule targeting holds many advantages,
333 including delivery, with development of reproducible and straightforward synthesis methods
334 allowing for future large-scale manufacturing and distribution. In recent years, several small
335 molecules have been reported to inhibit the IGF2BP family of proteins, either by binding directly,
336 or by decreasing expression of the protein. Perhaps the earliest inhibitor reported was an
337 isocorydine derivative, 8-amino-ICD, which was reported to target hepatocellular carcinoma and
338 decrease IGF2BP3 expression at $EC_{50}$ of 20 μM or greater (23). In non-small cell lung cancer, it
339 has been found that isoliquiritigenin is also able to down-regulate IGF2BP3 expression in a dose-
340 dependent manner (24). Another inhibitor, BTYNB, was reported to target IGF2BP1 in the 5-10
341 μM range (25). In the last few years, several inhibitors have been reported to target IGF2BP2 at
342 a range of concentrations in acute T-lymphoblastic leukemia and acute myeloid leukemia (13,26),
343 including CWI1-2 (sub-micromolar $IC_{50}$ in AML cell lines) and JX1(10-20 μM $IC_{50}$). Most recently,
344 a virtual screening approach identified AE-848 as an inhibitor of IGF2BP3 with an $IC_{50}$ of ~10-40
345 μM in ovarian cancer (27). Hence, the targeting of IGF2BP family proteins is of great interest in
346 the field, but to date, there are no small molecules in clinical use or in the clinical trial pipeline to
347 target IGF2BP3. Our discoveries here indicate that I3IN-002 is the most potent inhibitor of
348 IGF2BP3 reported to date, which provides the impetus for further drug discovery efforts.
349
350 Biologically active small molecules containing indolyltriazine cores possess potent and selective
351 activity across a variety of indications. Other anti-cancer compounds containing the motif include
352 an inhibitor of tyrosine phosphatase SHP-2(28), and a commercially available tool compound,
353 Inauhzin, which acts as a SIRT-1 inhibitor (29). Further, this motif has been also found in
354 antibiotics, α-glucosidase inhibitors, and targeted p-glycoprotein inhibitors, amongst other classes
355 of biologically relevant molecules (30-33). Notably, many of these compounds are demonstrated

356 to be highly selective. This relatively diverse set of targets is consistent with our findings that small
357 changes in the structure can markedly alter the bioactivity of the indolyltriazine in acute leukemia
358 (i.e., only 2 out of 29 TR-FRET-active indolyltriazine compounds tested showed bioactivity). In
359 other words, the specificity of the compounds may be highly malleable with chemical modifications
360 of the side chains. Based these data, we have some early indications of structural constraints on
361 compounds that might be viable biologically. Our initial efforts indicate that I3IN-002 can be readily
362 synthesized using widely commercially available component molecules. This information should
363 enable future efforts to develop compound analogs of I3IN-002 that display selective binding to
364 IGF2BP3, without off-target effects. Importantly, while the indolyltriazine is seemingly privileged
365 with respect to bioactivity, it is not found in any commercially available drugs to date.
366
367 It is also of interest to note that we recently showed that IGF2BP3 genetic ablation was additive
368 with menin inhibition in MLL-AF4 leukemia (14). MLL-AF4 leads to a dramatic dysregulation of
369 transcription driven by inappropriate recruitment of elements of the super elongation complex to
370 areas bound by MLL(34). Hence, an RNA binding protein may be particularly important in this
371 context. While outside the scope of this report, compounds generated here could therefore be
372 useful in combinatorial therapeutic approaches with menin inhibition. It should be noted here that
373 recent work claimed a somewhat contradictory role for IGF2BP3 in stabilizing MLL fusion
374 transcripts, perhaps due to significantly different models and readouts used in the paper (35).
375 Nonetheless, IGF2BP3 targets include a number of key oncogenic proteins, which are themselves
376 the targets of advanced small molecule development programs. For example, CDK6 is a direct
377 target of IGF2BP3 that is upregulated by the latter's activity, and anti-CDK4/6 inhibitors have been
378 developed as potent agents in cancer therapy, for example, in breast cancer (36). BCL2 is also
379 a direct target of IGF2BP3, and the BCL2 inhibitor Venetoclax has shown activity in a number of
380 hematologic malignancies, including B-ALL and AML. Other targets, such as MYC, which have

381 long been elusive are also now being actively pursued with small molecule approaches (37).
382 Hence, our development of small molecule inhibitors could be especially important in future
383 combinatorial therapy approaches, and is an important future direction for our work.
384
385 While this work contains important advances, we acknowledge limitations of our study. Despite
386 exhaustive attempts, efforts to produce large quantities of full-length, untagged proteins have thus
387 far been unsuccessful, limiting our ability to perform detailed binding affinity measurements. We
388 believe this may be due to intrinsic properties of the protein, which is known to be present in stress
389 granules and undergo phase separation (57). While we see evidence of protein-compound
390 binding, we have thus far not been able to quantify the strength of binding in vitro. Moreover, off-
391 target effects cannot yet be ruled out and pharmacological properties will need to be optimized.
392 Thus, future directions will involve analog synthesis and biochemical evaluation to ultimately
393 improve and validate selective binding to IGF2BP3, while also optimizing drug-like properties.
394
395 Overall, our study has led to the discovery and validation of I3IN-002, a small molecule that inhibits
396 IGF2BP3. While our work has thus far focused on the role of IGF2BP3 in acute leukemia, it is
397 estimated that up to 15% of all human cancers overexpress IGF2BP3, based on the COSMIC
398 database, and there are several excellent reviews on this topic (3,18,38). This includes a number
399 of distinct epithelial malignances and subtypes of hematolymphoid cancer (39-46). Knockdown of
400 IGF2BP3 inhibits cancer cell growth, motility and features of aggressive cancer in a variety of
401 cancer subtypes (8,44,47,48). The IGF2BP3 protein shows a pattern of expression consistent
402 with an “oncofetal protein”(49), with very low to absent expression in adult tissues. Consistent
403 with this notion, our work has determined that IGF2BP3 appears to be largely dispensable in
404 homeostatic development (6), providing a significant therapeutic window for targeting. It should
405 be noted that IGF2BP3 expression is quite variable within different cancer types, and hence,

406 future indications would need to be carefully defined. We speculate that IGF2BP3 expression
407 could be evaluated in different cancer types by widely available techniques such as
408 immunohistochemistry; and compounds such as I3IN-002, or future derivatives could be
409 administered as a precision medicine intervention in carefully selected patients. Hence, I3IN-002
410 serves as a promising lead compound for future drug discovery efforts aimed at identifying
411 selective inhibitors of IGF2BP3, particularly for the treatment of acute leukemia.

412 **METHODS**

413 **A complete description of methods can be found in Supplementary Information.**

414 **Cell lines and cell culture**

415 All cell lines were maintained in standard condition in incubator at 37 °C and 5% $CO_2$. Human B-
416 ALL cell lines, RS4;11 (ATCC CRL-1873), NALM6 (ATCC CRL-3273), SEM (DMZ-ACC 546),
417 PER785 , REH (ATCC CRL-8286 ), and KASUMI-2 (DSMZ ACC 526), and immortalized MLL-Af4
418 transformed murine HSPCs were cultured as previously described (15). A full listing of reagents
419 is provided in **Supp. Table 1**.

420

421 **Antibodies.** Antibodies were used for Western blotting, FACS, and immunoprecipitation
422 experiments as described (4,6,14,15). A list of antibodies is provided in Supp. Table 2.

423

424 **Protein Purification and High throughput assays.**

425 IGF2BP3-GFP-Flag over-expression plasmid was constructed by fusing full length IGF2BP3 CDS
426 with GFP CDS and Flag CDS and cloned in pCDNA 3.0 vector. Protein was purified using
427 standard methods and anti-Flag based affinity purification. Purified protein was added to pre-
428 incubated Streptavidin-terbium plus biotinylated m6A-labeled RNA oligonucleotide (**Supp. Table**
429 **4**). The plate was incubated for 1 hr. at RT for binding and read on EnVision microplate reader
430 (Perkin Elmer) with a dual PMT configuration using a 340 nm excitation and a dual emission mirror
431 block with using a 495 nm emission filter for Terbium fluorescence (W1 channel) and a 525 nm
432 emission filter for GFP fluorescence (W2 channel). The assay was miniaturized to 10uL in 384-
433 well plates and an in-house compound deck at UCLA MSSR was applied to the assay, with
434 parameters as described in Results. Data analysis was performed as described in Supplementary
435 Methods to identify a preliminary list of hits.

436

437 **Counter-Screen and Cell-based Assays.**

438 Wild type and IGF2BP3-deleted SEM cell lines (14) were treated with compound, grown for 4
439 days under normal growth conditions, and assayed for cell growth in 384-well plates with CellTiter-
440 Glo, a luminescence-based reagent described previously (6,14,15). Following identification of
441 lead compounds, further measurements of apoptosis, cell cycle and proliferation were performed
442 as we have previously described(6,14,15).

443

444 **Compound Synthesis.** Briefly, organic synthesis was performed based on utilizing
445 commercially available fragments and a custom in-house strategy allowing for the design of he
446 original compound and future analogs. Full description is provided in the Supplementary
447 Methods.

448

449 **Assays to define on-target activity.**

450 A cellular thermal shift assay was performed on SEM cells treated with the test compound, based
451 on published protocols with minor modifications described in the Supplemental methods (50).
452 Thermal shift assay with purified protein, and Drug Affinity responsive target stability assays were
453 performed as previously described (51,52). Lastly, RNA immunoprecipitation and RNA-
454 sequencing were performed as we have described in prior publications(4,14).

455

456 **Animal Experiments**

457 For in vivo studies, C57BL/6J, B6.SJL-*Ptprc*$^{a}$ *Pepc*$^{b,}$/BoyJ (B6 CD45.1), and B6J.129(Cg)-
458 Gt(ROSA)26Sor$^{tm1.1(CAG\text{-}cas9_{*},\text{-}EGFP)Fezh/J}$ (Cas9-GFP, BL/6J) were procured from The Jackson
459 Laboratory. Preliminary toxicity studies were carried out to identify issues with small molecule
460 delivery in non-transplanted mice. Primary murine leukemia cells (WT and Igf2bp3 KO) as
461 previously described (14) were transplanted into busulfan-conditioned recipients. Dosing was

462 carried out intraperitoneally, 3 times a week for three weeks. Once the peripheral blood
463 engraftment reached >20% at 4 weeks, the experiment was terminated and tissues were
464 harvested to be analyzed by FACS, histology and RT-qPCR. A separate experiment examined
465 overall and leukemia free survival. All of the animal experiments received Institutional Animal
466 Research Committee approval at UCLA.

**ACKNOWLEDGMENTS**

We thank Dr. Stuart Conway and Keefe Oei for helpful conversations, advice and protocols for biophysical assays. We thank members of the Rao lab, particularly, Jaspal Bassi and Tiffany Tran, as well as Dr. John Colicelli, for helpful discussions regarding the research. This work was supported by CIRM DISC-2-13456 from the California Institute of Regenerative Medicine (DSR), R01CA264986 from the National Institutes of Health (DSR, JRS), R03CA251854 (DSR), the Jonsson Comprehensive Cancer Center (JCCC) (DSR), the Gary & Barbara Luboff Mitzvah Fund (DSR) and the UCLA Innovation Fund Award (DSR). Flow cytometry was performed in the UCLA JCCC and Center for AIDS Research Flow Cytometry Core Facility that is supported by National Institutes of Health awards AI28697, and award number P30CA016042, the JCCC, the UCLA AIDS Institute, and the David Geffen School of Medicine at UCLA. We are especially indebted to the Molecular Screening Shared Resource team for setup and execution of all small molecule related in vitro assays. The MSSR is also supported by the Jonsson Comprehensive Cancer Center (NIH award number P30CA016042, Cancer Center Support Grant).These studies were supported by the National Science Foundation (DGE-2034835 for GMS and DGE-1650604 for MMM). These studies were supported by shared instrumentation grants from the NSF (CHE-1048804), the National Center for Research Resources (S10RR025631), and the NIH Office of Research Infrastructure Programs (S10OD028644).

485 **AUTHOR CONTRIBUTIONS**

486 A.K.J.: Designed research, Performed experiments, Acquired data, Analyzed data, Generated
487 Figures, Wrote manuscript, Experimental Lead

488 G.M.S.: Performed experiments, Acquired data, Analyzed data, Assisted in generating figures

489 M.L.T.: Performed experiments, Acquired data, Analyzed data

490 J.P.S.: Performed experiments, Acquired data, Analyzed data

491 C.Y.: Performed experiments

492 M.M.M.: Performed experiments, Acquired data, Analyzed data

493 G.S.: Performed experiments

494 T.M.T.: Performed experiments

495 T.L.L.: Performed experiments, Acquired data

496 A.C.: Performed experiments, Acquired data

497 A.J.R.: Analyzed data

498 J.R.S.: Analyzed data

499 R.S.K.: Provided MLL AF4 B-ALL cell line

500 R.D.D.: Designed research, Analyzed data

501 N.K.G.: Designed research, Analyzed data, Edited manuscript

502 D.S.R.: Designed research, Analyzed data, Wrote manuscript, Secured Funding, Project leader

503 **CONFLICTS OF INTEREST**

504 DSR has served as a consultant to AbbVie, a pharmaceutical company that develops and markets
505 drugs for hematologic disorders. AKJ, MLT, GMS, JPS, RDD, NKG and DSR are inventors on a
506 patent application that includes the compound I3IN-002.

507 **References**


508 1. Müeller-Pillasch F, Lacher U, Wallrapp C, Micha A, Zimmerhackl F, Hameister H, et al.
509 Cloning of a gene highly overexpressed in cancer coding for a novel KH-domain containing
510 protein. Oncogene 1997;14(22):2729-33.
511 2. Nielsen J, Christiansen J, Lykke-Andersen J, Johnsen AH, Wewer UM, Nielsen FC. A family
512 of insulin-like growth factor II mRNA-binding proteins represses translation in late
513 development. Molecular and cellular biology 1999;19(2):1262-70.
514 3. Mancarella C, Scotlandi K. IGF2BP3 From Physiology to Cancer: Novel Discoveries,
515 Unsolved Issues, and Future Perspectives. Frontiers in Cell and Developmental Biology
516 2020;7(363).
517 4. Palanichamy JK, Tran TM, Howard JM, Contreras JR, Fernando TR, Sterne-Weiler T, et al.
518 RNA-binding protein IGF2BP3 targeting of oncogenic transcripts promotes hematopoietic
519 progenitor proliferation. J Clin Invest 2016;126(4):1495-511.
520 5. Stoskus M, Gineikiene E, Valceckiene V, Valatkaite B, Pileckyte R, Griskevicius L.
521 Identification of characteristic IGF2BP expression patterns in distinct B-ALL entities. Blood
522 Cells, Molecules, and Diseases 2011;46(4):321-26.
523 6. Tran TM, Philipp J, Bassi JS, Nibber N, Draper JM, Lin TL, et al. The RNA-binding protein
524 IGF2BP3 is critical for MLL-AF4-mediated leukemogenesis. Leukemia 2022;36(1):68-79.
525 7. Lin S, Luo RT, Ptasinska A, Kerry J, Assi SA, Wunderlich M, et al. Instructive Role of MLL-
526 Fusion Proteins Revealed by a Model of t(4;11) Pro-B Acute Lymphoblastic Leukemia.
527 Cancer Cell 2016;30(5):737-49.
528 8. Yang Z, Wang T, Wu D, Min Z, Tan J, Yu B. RNA N6-methyladenosine reader IGF2BP3
529 regulates cell cycle and angiogenesis in colon cancer. J Exp Clin Cancer Res
530 2020;39(1):203.
531 9. Huang H, Weng H, Sun W, Qin X, Shi H, Wu H, et al. Recognition of RNA N(6)-
532 methyladenosine by IGF2BP proteins enhances mRNA stability and translation. Nat Cell
533 Biol 2018;20(3):285-95.
534 10. Ren F, Lin Q, Gong G, Du X, Dan H, Qin W, et al. Igf2bp3 maintains maternal RNA stability
535 and ensures early embryo development in zebrafish. Communications Biology
536 2020;3(1):94.
537 11. Gao S, Gu Y, Niu S, Wang Y, Duan L, Pan Y, et al. DMDRMR-mediated regulation of m6A-
538 modified CDK4 by m6A reader IGF2BP3 drives ccRCC progression. Cancer Research
539 2020:canres.1619.2020.
540 12. Elcheva IA, Spiegelman VS. Targeting RNA-binding proteins in acute and chronic leukemia.
541 Leukemia 2020.
542 13. Weng H, Huang F, Yu Z, Chen Z, Prince E, Kang Y, et al. The m(6)A reader IGF2BP2 regulates
543 glutamine metabolism and represents a therapeutic target in acute myeloid leukemia.
544 Cancer Cell 2022;40(12):1566-82.e10.
545 14. Lin TL, Jaiswal AK, Ritter AJ, Reppas J, Tran TM, Neeb ZT, et al. Targeting IGF2BP3 enhances
546 antileukemic effects of menin-MLL inhibition in MLL-AF4 leukemia. Blood Adv
547 2024;8(2):261-75.

548 15. Jaiswal AK, Truong H, Tran TM, Lin TL, Casero D, Alberti MO, et al. Focused CRISPR-Cas9
549 genetic screening reveals USO1 as a vulnerability in B-cell acute lymphoblastic leukemia.
550 Scientific Reports 2021;11(1):13158.
551 16. Rahim F, Ullah K, Ullah H, Wadood A, Taha M, Ur Rehman A, et al. Triazinoindole analogs
552 as potent inhibitors of α-glucosidase: synthesis, biological evaluation and molecular
553 docking studies. Bioorg Chem 2015;58:81-7.
554 17. Shelke SM, Bhosale SH. Synthesis, antidepressant evaluation and QSAR studies of novel
555 2-(5H-[1,2,4]triazino[5,6-b]indol-3-ylthio)-N-(substituted phenyl)acetamides. Bioorg Med
556 Chem Lett 2010;20(15):4661-4.
557 18. Bell JL, Wächter K, Mühleck B, Pazaitis N, Köhn M, Lederer M, et al. Insulin-like growth
558 factor 2 mRNA-binding proteins (IGF2BPs): post-transcriptional drivers of cancer
559 progression? Cell Mol Life Sci 2013;70(15):2657-75.
560 19. Wang E, Lu SX, Pastore A, Chen X, Imig J, Chun-Wei Lee S, et al. Targeting an RNA-Binding
561 Protein Network in Acute Myeloid Leukemia. Cancer Cell 2019;35(3):369-84.e7.
562 20. Gebauer F, Schwarzl T, Valcárcel J, Hentze MW. RNA-binding proteins in human genetic
563 disease. Nature Reviews Genetics 2021;22(3):185-98.
564 21. Tran TM, Rao DS. RNA binding proteins in MLL-rearranged leukemia. Exp Hematol Oncol
565 2022;11(1):80.
566 22. Jaiswal AK, Thaxton ML, Scherer GM, Sorrentino JP, Garg NK, Rao DS. Small molecule
567 inhibition of RNA binding proteins in haematologic cancer. RNA Biology 2024;21(1):1-14.
568 23. Li M, Zhang L, Ge C, Chen L, Fang T, Li H, et al. An isocorydine derivative (d-ICD) inhibits
569 drug resistance by downregulating IGF2BP3 expression in hepatocellular carcinoma.
570 Oncotarget 2015;6(28):25149-60.
571 24. Cui Y, Wu Y, Wang C, Wang Z, Li Y, Jiang Z, et al. Isoliquiritigenin inhibits non-small cell
572 lung cancer progression via m6A/IGF2BP3-dependent TWIST1 mRNA stabilization.
573 Phytomedicine 2022;104:154299.
574 25. Mahapatra L, Andruska N, Mao C, Le J, Shapiro DJ. A Novel IMP1 Inhibitor, BTYNB, Targets
575 c-Myc and Inhibits Melanoma and Ovarian Cancer Cell Proliferation. Transl Oncol
576 2017;10(5):818-27.
577 26. Dahlem C, Abuhaliema A, Kessler SM, Kröhler T, Zoller BGE, Chanda S, et al. First Small-
578 Molecule Inhibitors Targeting the RNA-Binding Protein IGF2BP2/IMP2 for Cancer Therapy.
579 ACS Chem Biol 2022;17(2):361-75.
580 27. Shu C, Gu MH, Zeng C, Shao WG, Li HY, Ma XH, et al. Small-molecule exhibits anti-tumor
581 activity by targeting the RNA m(6)A reader IGF2BP3 in ovarian cancer. Am J Cancer Res
582 2023;13(10):4888-902.
583 28. Yu W-M, Guvench O, MacKerell AD, Jr., Qu C-K. Identification of Small Molecular Weight
584 Inhibitors of Src Homology 2 Domain-Containing Tyrosine Phosphatase 2 (SHP-2) via in
585 Silico Database Screening Combined with Experimental Assay. Journal of Medicinal
586 Chemistry 2008;51(23):7396-404.
587 29. Zhang Q, Zeng SX, Zhang Y, Zhang Y, Ding D, Ye Q, et al. A small molecule Inauhzin inhibits
588 SIRT1 activity and suppresses tumour growth through activation of p53. EMBO Molecular
589 Medicine 2012;4(4):298-312-12.

590 30. Li H, Liu J, Liu C-F, Li H, Luo J, Fang S, et al. Design, Synthesis, and Biological Evaluation of
591 Membrane-Active Bakuchiol Derivatives as Effective Broad-Spectrum Antibacterial
592 Agents. Journal of Medicinal Chemistry 2021;64(9):5603-19.
593 31. Garzan A, Willby MJ, Ngo HX, Gajadeera CS, Green KD, Holbrook SYL, et al. Combating
594 Enhanced Intracellular Survival (Eis)-Mediated Kanamycin Resistance of Mycobacterium
595 tuberculosis by Novel Pyrrolo[1,5-a]pyrazine-Based Eis Inhibitors. ACS Infectious Diseases
596 2017;3(4):302-09.
597 32. Rahim F, Ullah K, Ullah H, Wadood A, Taha M, Rehman AU, et al. Triazinoindole analogs
598 as potent inhibitors of α-glucosidase: Synthesis, biological evaluation and molecular
599 docking studies. Bioorganic Chemistry 2015;58:81-87.
600 33. Wise JG, Nanayakkara AK, Aljowni M, Chen G, De Oliveira MC, Ammerman L, et al.
601 Optimizing Targeted Inhibitors of P-Glycoprotein Using Computational and Structure-
602 Guided Approaches. Journal of Medicinal Chemistry 2019;62(23):10645-63.
603 34. Lin C, Smith ER, Takahashi H, Lai KC, Martin-Brown S, Florens L, et al. AFF4, a Component
604 of the ELL/P-TEFb Elongation Complex and a Shared Subunit of MLL Chimeras, Can Link
605 Transcription Elongation to Leukemia. Molecular Cell 2010;37(3):429-37.
606 35. Okuda H, Miyamoto R, Takahashi S, Kawamura T, Ichikawa J, Harada I, et al. RNA-binding
607 proteins of KHDRBS and IGF2BP families control the oncogenic activity of MLL-AF4. Nat
608 Commun 2022;13(1):6688.
609 36. Wolff AC. CDK4 and CDK6 Inhibition in Breast Cancer — A New Standard. New England
610 Journal of Medicine 2016;375(20):1993-94.
611 37. Boike L, Cioffi AG, Majewski FC, Co J, Henning NJ, Jones MD, et al. Discovery of a
612 Functional Covalent Ligand Targeting an Intrinsically Disordered Cysteine within MYC. Cell
613 Chem Biol 2021;28(1):4-13.e17.
614 38. Lederer M, Bley N, Schleifer C, Hüttelmaier S. The role of the oncofetal IGF2 mRNA-
615 binding protein 3 (IGF2BP3) in cancer. Seminars in Cancer Biology 2014;29:3-12.
616 39. Yantiss RK, Woda BA, Fanger GR, Kalos M, Whalen GF, Tada H, et al. KOC (K homology
617 domain containing protein overexpressed in cancer): a novel molecular marker that
618 distinguishes between benign and malignant lesions of the pancreas. The American
619 journal of surgical pathology 2005;29(2):188-95.
620 40. Schaeffer DF, Owen DR, Lim HJ, Buczkowski AK, Chung SW, Scudamore CH, et al. Insulin-
621 like growth factor 2 mRNA binding protein 3 (IGF2BP3) overexpression in pancreatic
622 ductal adenocarcinoma correlates with poor survival. BMC Cancer 2010;10:59.
623 41. Kobel M, Xu H, Bourne PA, Spaulding BO, Shih Ie M, Mao TL, et al. IGF2BP3 (IMP3)
624 expression is a marker of unfavorable prognosis in ovarian carcinoma of clear cell subtype.
625 Mod Pathol 2009;22(3):469-75.
626 42. Suvasini R, Shruti B, Thota B, Shinde SV, Friedmann-Morvinski D, Nawaz Z, et al. Insulin
627 growth factor-2 binding protein 3 (IGF2BP3) is a glioblastoma-specific marker that
628 activates phosphatidylinositol 3-kinase/mitogen-activated protein kinase (PI3K/MAPK)
629 pathways by modulating IGF-2. J Biol Chem 2011;286(29):25882-90.
630 43. Lochhead P, Imamura Y, Morikawa T, Kuchiba A, Yamauchi M, Liao X, et al. Insulin-like
631 growth factor 2 messenger RNA binding protein 3 (IGF2BP3) is a marker of unfavourable
632 prognosis in colorectal cancer. Eur J Cancer 2012;48(18):3405-13.

633 44. Schmiedel D, Tai J, Yamin R, Berhani O, Bauman Y, Mandelboim O. The RNA binding
634 protein IMP3 facilitates tumor immune escape by downregulating the stress-induced
635 ligands ULPB2 and MICB. Elife 2016;5.
636 45. King RL, Pasha T, Roullet MR, Zhang PJ, Bagg A. IMP-3 is differentially expressed in normal
637 and neoplastic lymphoid tissue. Hum Pathol 2009;40(12):1699-705.
638 46. Forbes SA, Beare D, Gunasekaran P, Leung K, Bindal N, Boutselakis H, et al. COSMIC:
639 exploring the world's knowledge of somatic mutations in human cancer. Nucleic acids
640 research 2015;43(D1):D805-D11.
641 47. Jønson L, Christiansen J, Hansen Thomas VO, Vikeså J, Yamamoto Y, Nielsen Finn C. IMP3
642 RNP Safe Houses Prevent miRNA-Directed HMGA2 mRNA Decay in Cancer and
643 Development. Cell Reports 2014;7(2):539-51.
644 48. Xu W, Sheng Y, Guo Y, Huang Z, Huang Y, Wen D, et al. Increased IGF2BP3 expression
645 promotes the aggressive phenotypes of colorectal cancer cells in vitro and vivo. J Cell
646 Physiol 2019;234(10):18466-79.
647 49. Degrauwe N, Suvà M-L, Janiszewska M, Riggi N, Stamenkovic I. IMPs: an RNA-binding
648 protein family that provides a link between stem cell maintenance in normal development
649 and cancer. Genes & Development 2016;30(22):2459-74.
650 50. Jafari R, Almqvist H, Axelsson H, Ignatushchenko M, Lundbäck T, Nordlund P, et al. The
651 cellular thermal shift assay for evaluating drug target interactions in cells. Nature
652 Protocols 2014;9(9):2100-22.
653 51. Pai MY, Lomenick B, Hwang H, Schiestl R, McBride W, Loo JA, et al. Drug affinity responsive
654 target stability (DARTS) for small-molecule target identification. Methods Mol Biol
655 2015;1263:287-98.
656 52. Wu T, Hornsby M, Zhu L, Yu JC, Shokat KM, Gestwicki JE. Protocol for performing and
657 optimizing differential scanning fluorimetry experiments. STAR Protoc 2023;4(4):102688.
658 58. Schneider T, Hung LH, Aziz M, Wilmen A, Thaum S, Wagner J, Janowski R, Müller S,
659 Schreiner S, Friedhoff P, Hüttelmaier S, Niessing D, Sattler M, Schlundt A, Bindereif A.
660 Combinatorial recognition of clustered RNA elements by the multidomain RNA-binding
661 protein IMP3. Nat Commun. 2019 May 22;10(1):2266. doi: 10.1038/s41467-019-09769-8.
662

663 **FIGURE LEGENDS**

664 **Figure 1. Design and execution of a high throughput assay to identify small molecule**
665 **inhibitors of IGF2BP3.**

666 a. Schematic of assay. IGF2BP3-GFP fusion protein is bound to an $m^6A$-modified, biotinylated
667 RNA oligonucleotide, which in turn is bound to Streptavidin Terbium (SA-Tb). Förster resonance
668 energy transfer occurs when the protein and RNA are bound.

669 b. GFP Fluorescence (fold over control) plotted for different combinations of Streptavidin Terbium
670 (SA-Tb), IGF2BP3-GFP (I3-GFP), m6A-modified RNA (m6A RNA) or unmethylated, biotinylated
671 RNA (RNA).

672 c. GFP Fluorescence (arbitrary units) as a function of IGF2BP3-GFP protein concentration.

673 d. High throughput screening assay Z'-scores for control reactions across 600+ plates screening
674 over 186,978 compounds.

675 e. Screening was conducted first with a limited set of compounds (preliminary screen) prior to a
676 full-scale screen. Fluorescence ratios were calculated as W1/W2 where W1 is the Terbium
677 fluorescence and W2 is the GFP fluorescence. Shown are the percent of compounds satisfying a
678 single criterion (i.e., Ratio Z) or two criteria (Ratio Z and W1 Z).

679 f. First "core structure" identified from the screen. The indolyltriazine substructure was conserved
680 across multiple hits from screening in d and e.

681 g. Comparison of total number of hits in the library, versus hits amongst compounds containing
682 the first core structure; Fisher's exact test, $p<0.0001$.

683

684 **Figure 2. Identification of molecules with biochemical activity and IGF2BP3-dependent**
685 **anti-proliferative properties.**

686 a. Counter-screen strategy: SEM cells with (SEM-WT) and without IGF2BP3 (SEM-I3KO) are
687 treated in a medium-throughput format with the small molecules identified from the biochemical

688 screen.

689 b. Scatter plot examining the relationship between relative changes in cell growth, measured by
690 CellTiterGlo and normalized to DMSO control, in SEM-WT (x-axis) and SEM-I3KO (y-axis).
691 Compounds *1*, *2* and *3* (red-brown) were noted to have a preferential effect on SEM-WT and a
692 lesser effect in SEM-I3KO. Cells were treated with 5 μM solutions of test compounds.

693 c-e. Structures of compounds *1*, *2* and *3* (top) and corresponding concentration dependent
694 changes in cell growth rate (bottom) for the three compounds with favorable characteristics on
695 screening. Growth rate was measured using CellTiterGlo and normalized to DMSO control in
696 SEM-WT cell line.

697

698 **Figure 3. I3IN-002 alters cell growth, cell cycle, and apoptosis in human and mouse**
699 **leukemic cells.**

700 a. Chemical synthesis of **I3IN-002**.

701 b. IC50 values of I3IN-002 on MLLr B-ALL and B-ALL cell lines.

702 c-e. Concentration-dependent alterations of cell growth curves over 4 days of cell culture with
703 I3IN-002 treatment, assessed by CellTiterGlo assay, and plotted as relative luminescence units
704 (RLU). SEM (c), RS4;11 (d), and Lin-/MLL-Af4 (e) cells were assayed in this experiment. Data
705 represent mean and standard error of mean in 8 replicates.

706 f. Measurement of SubG0 cells by propidium iodide staining in SEM and RS4;11 cells,
707 respectively, following treatment with 5 μM I3IN-002 or DMSO. Data represents mean and
708 standard error of mean of the calculated percentage of cells at each stage of cell cycle with 3
709 replicates.

710 g. Measurement of apoptosis induction, by Caspase 3/7 activity assay in SEM cells. Data
711 represents mean and standard error of mean with 8 replicates.

712 h. Measurement of cell death by orthogonal method of Annexin V and propidium iodide staining
713 in SEM cells. Shown are the % of cells that are single or double positive for propidium iodide and
714 Annexin V.
715 i. Quantitation of a leukemic stem-cell enriched population by assaying the CD34+ c-kit+
716 population following in vitro treatment of Lin-/MLL-Af4 cells in culture.
717 j. Measurement of colony formation in methylcellulose following treatment of a murine model of
718 MLL-Af4 driven leukemia (14,15) with I3IN-002. Data represents the mean number of total
719 colonies for each condition, with 3 replicates per condition. I3KO represents genetic knockout of
720 IGF2BP3, which results in reduced colony formation
721 For Figure 3, statistical significance was evaluated by student's T-test, *$p<0.05$; **$p<0.01$;
722 ***$p<0.001$; ****$p<0.0001$.
723
724 **Figure 4. I3IN-002 inhibits leukemic growth in vivo.**
725 a. Schematic of mouse experiment.
726 b. Gross pathology photographs of murine spleens from mice syngeneically transplanted with Lin-
727 /MLL-Af4 cells. I3KO are genetic knockouts of IGF2BP3, which markedly reduced leukemic
728 engraftment.
729 c. Histology of liver (top) and spleen (bottom) from treated mice, as indicated. Arrow indicates a
730 leukemic infiltrate in the liver in the portal area. Dotted lines indicate splenic white pulp, with
731 leukemic infiltrates in the red pulp (area outside the dotted lines). Hematoxylin and eosin staining,
732 original magnification, 200X.
733 d. Splenic weights from treated mice, as indicated.
734 e. FACS staining for CD34 and c-kit in the spleen of treated mice, as indicated.
735 f-i. Quantification of overall leukemia engraftment and various leukemia subsets in the spleen.

736 j-k. Quantification of overall leukemia engraftment and various leukemia subsets in the bone
737 marrow.
738 l. Kaplan-Meier survival curve shows effect of I3IN-002 injection on overall survival in syngeneic
739 bone marrow transplant experiment.
740 Data in e-k represents one experiment composed of the following numbers of animals: Vehicle,
741 n=8; I3IN-002, n=7; I3KO, n=5. Statistical significance was evaluated by student's T-test,
742 *p<0.05; **p<0.01; ***p<0.001; ****p<0.0001.
743
744 **Figure 5. I3IN-002 shows on-target activity in leukemia cells.**
745 a. Western blot analysis of RNA immunoprecipitation samples following treatment of SEM cells
746 with 5 μM I3IN-002. Input represents the input cell lysate; IgG represents a control
747 immunoprecipitation with isotype control: and "IP" represents anti-IGF2BP3 immunoprecipitation.
748 b. Quantification of *CDK6* and *BCL2* RNA recovered from RNA immunoprecipitation experiments
749 with or without treatment with I3IN-002.
750 c-d. Cellular thermal shift assay; Western blots of IGF2BP3 and beta-actin are shown following
751 treatment of cells with I3IN-002 or DMSO control, followed by heat-mediated denaturation and
752 removal of denatured protein (c) and quantification of western blot (d).
753 e. Thermal shift assay using purified full length IGF2BP3 protein.
754 f. Volcano plots of differentially expressed genes with genetic IGF2BP3 knockout (left) and with
755 I3IN-002 treatment (top) in SEM cells, using DESeq analysis on RNA-sequencing data from SEM
756 cells treated with DMSO, I3IN-002 and SEM/I3KO.
757 g. Venn diagram of shared differentially expressed genes with IGF2BP3 knockout and I3IN-002
758 treatment in SEM cells. Hypergeometric test of overlap showed a p-value<$10^{-16}$.
759 h. GSEA analysis of the overlapped genes between I3KO and I3IN-002 treated cells.

760 i-n. RT-qPCR based confirmation of genes showing common differential regulation between I3IN-
761 002 treatment and genetic knockout of IGF2BP3 (I3KO). Data are shown as fold change, following
762 normalization to DMSO, with 3 replicate measurements per sample.
763 o. Western blot measurement of CDK6, and BCL2, which are known targets of IGF2BP3.

# Figure 1.

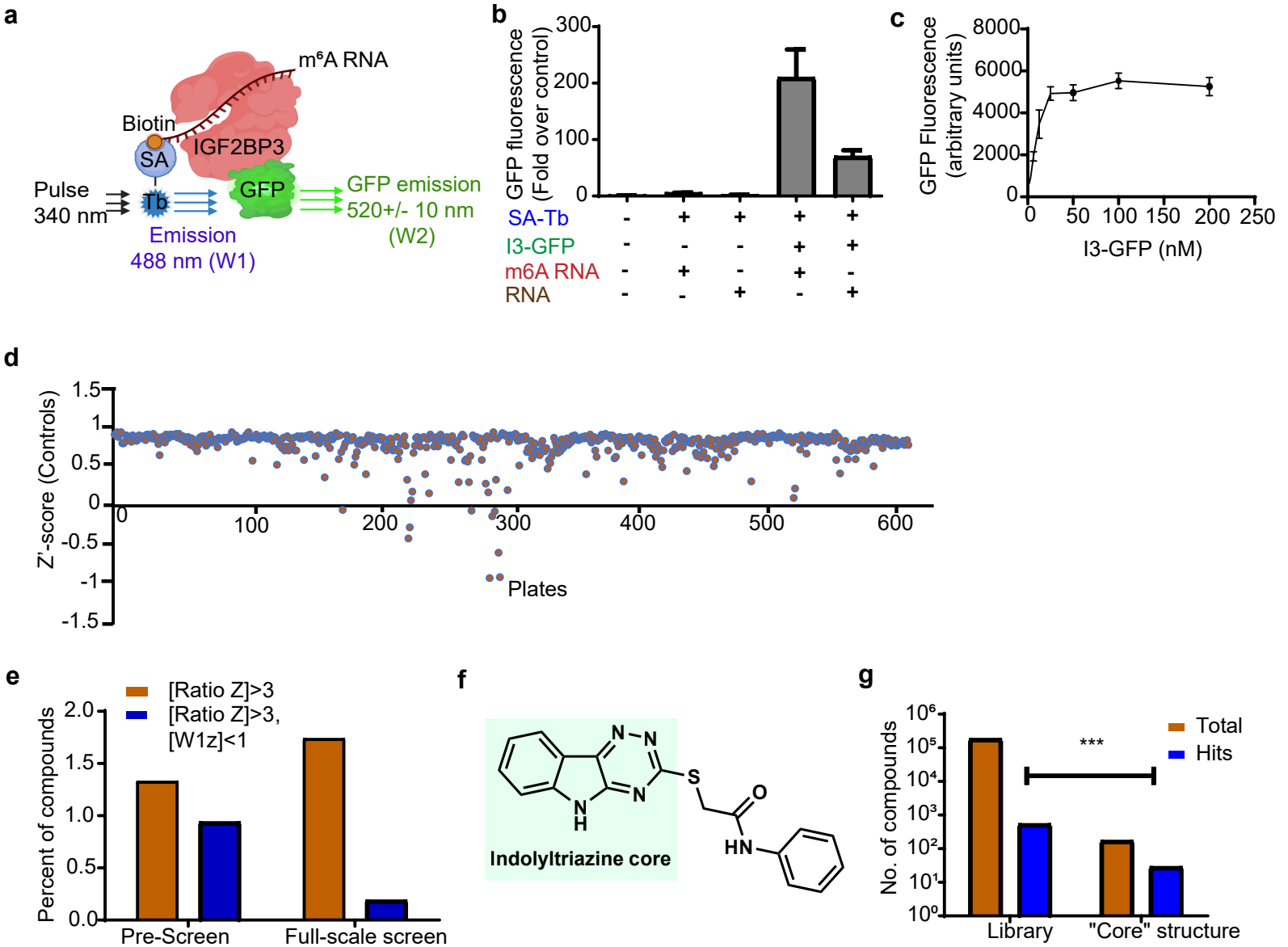
a
m6A RNA
Biotin
SA
IGF2BP3
Pulse
340 nm
Tb
GFP
GFP emission
520+/- 10 nm
(W2)
Emission
488 nm (W1)
b
GFP fluorescence
(Fold over control)
300
200
100
0
SA-Tb - + + + +
I3-GFP - - - + +
m6A RNA - + - + -
RNA - - + - +
c
GFP Fluorescence
(arbitrary units)
8000
6000
4000
2000
0
0 50 100 150 200 250
I3-GFP (nM)
d
Z'-score (Controls)
1.5
1
0.5
0
-0.5
-1
-1.5
0 100 200 300 400 500 600
Plates
e
[Ratio Z]>3
[Ratio Z]>3,
[W1z]<1
Percent of compounds
2.0
1.5
1.0
0.5
0.0
Pre-Screen
Full-scale screen
f
N
N
N
N
H
S
O
HN
Indolyltriazine core
g
No. of compounds
10^6
10^5
10^4
10^3
10^2
10^1
10^0
***
Total
Hits
Library
"Core" structure

# Figure 2.

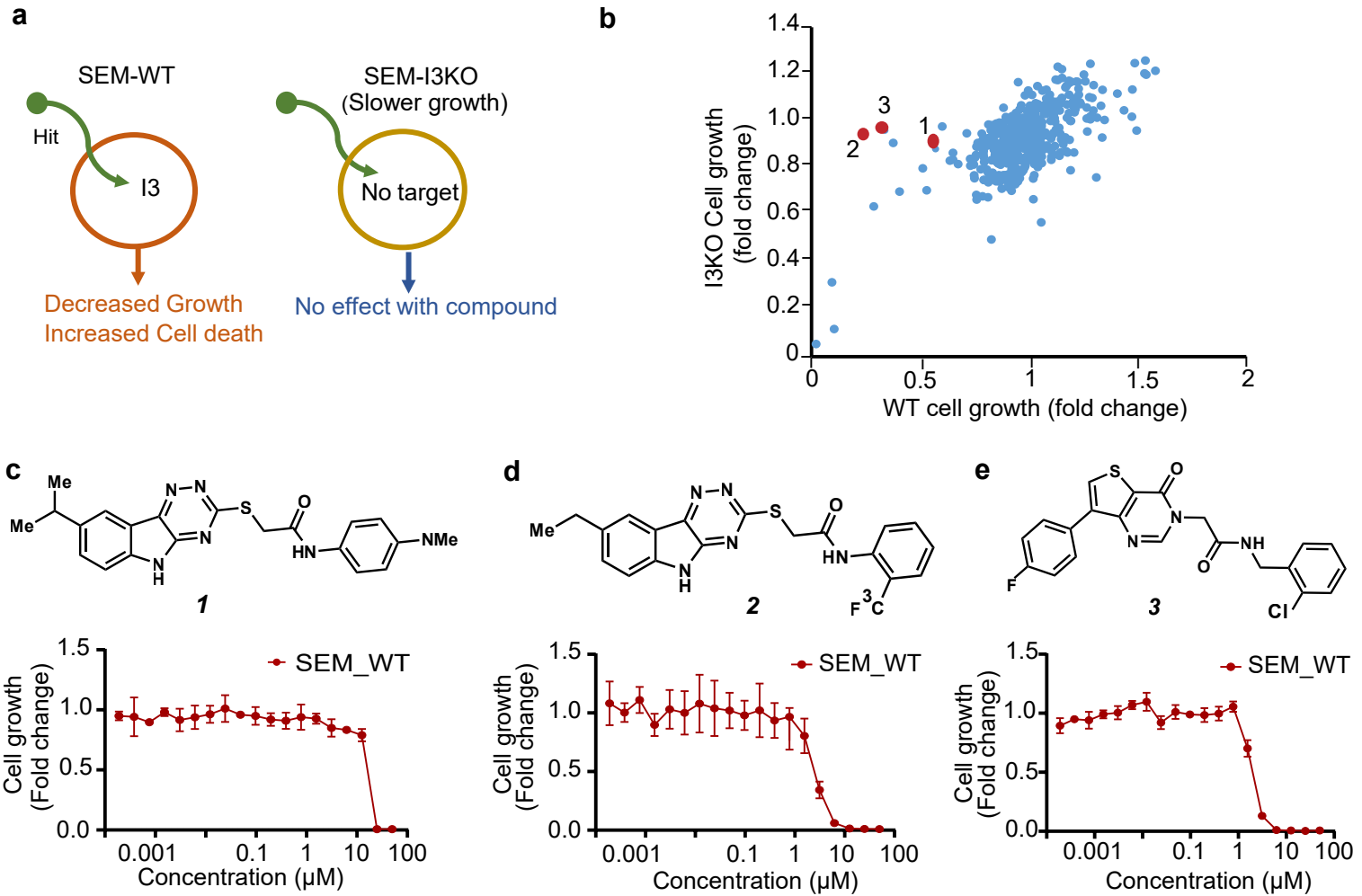
a
SEM-WT
Hit
I3
Decreased Growth
Increased Cell death
SEM-I3KO
(Slower growth)
No target
No effect with compound
b
I3KO Cell growth
(fold change)
WT cell growth (fold change)
1
2
3
c
d
e
1
2
3
SEM_WT
Cell growth
(Fold change)
Concentration (μM)

**Figure 3.**

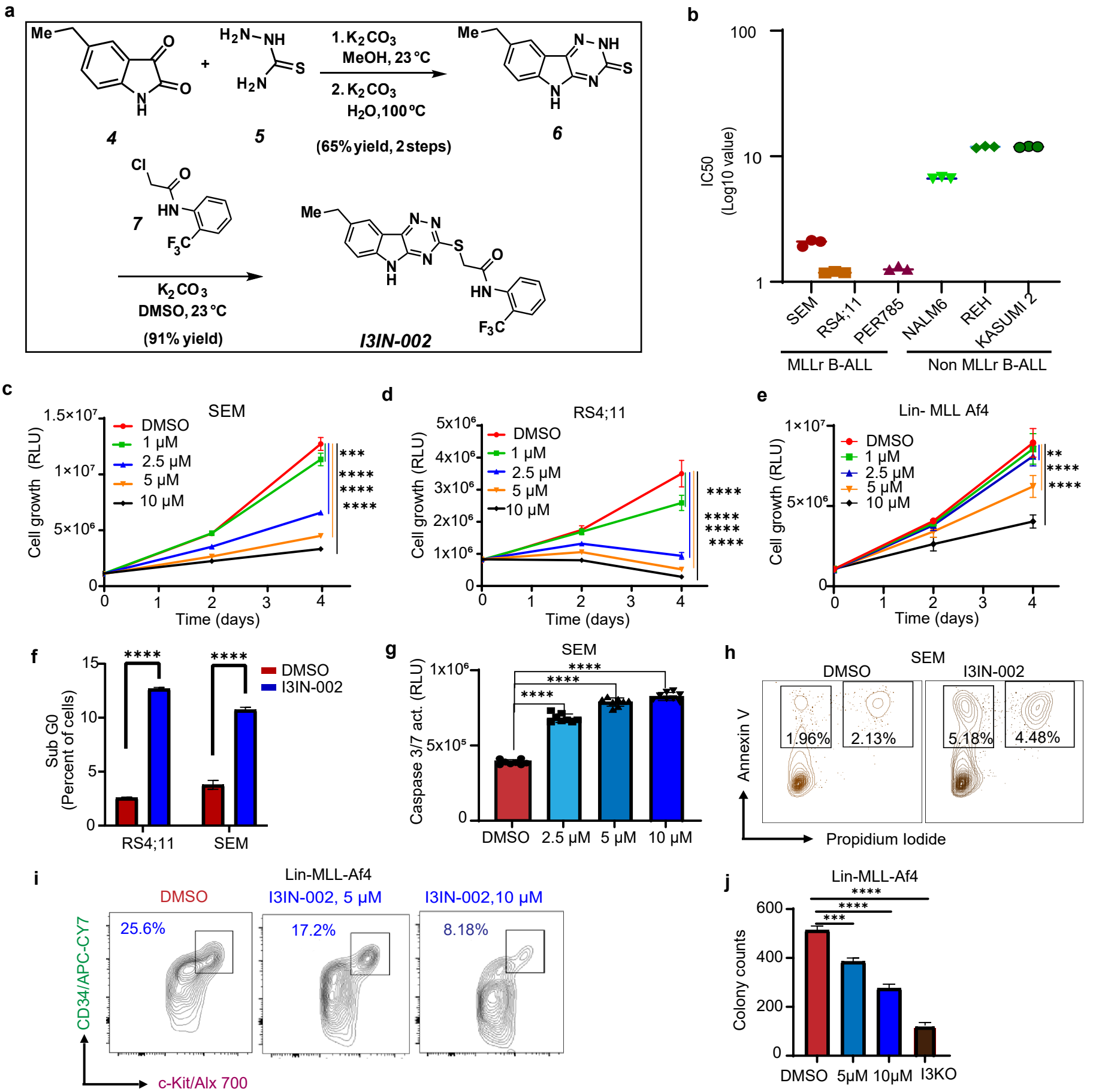
a
Me
4
5
1. K2CO3
MeOH, 23 °C
2. K2CO3
H2O, 100 °C
(65% yield, 2 steps)
6
7
K2CO3
DMSO, 23 °C
(91% yield)
I3IN-002
b
IC50 (Log10 value)
SEM
RS4;11
PER785
NALM6
REH
KASUMI 2
MLLr B-ALL
Non MLLr B-ALL
c
SEM
DMSO
1 μM
2.5 μM
5 μM
10 μM
Cell growth (RLU)
Time (days)
d
RS4;11
e
Lin- MLL Af4
f
Sub G0 (Percent of cells)
DMSO
I3IN-002
RS4;11
SEM
g
SEM
Caspase 3/7 act. (RLU)
DMSO
2.5 μM
5 μM
10 μM
h
SEM
DMSO
I3IN-002
1.96%
2.13%
5.18%
4.48%
Annexin V
Propidium Iodide
i
Lin-MLL-Af4
DMSO
I3IN-002, 5 μM
I3IN-002,10 μM
25.6%
17.2%
8.18%
CD34/APC-CY7
c-Kit/Alx 700
j
Lin-MLL-Af4
Colony counts
DMSO
5μM
10μM
I3KO

# Figure 4.

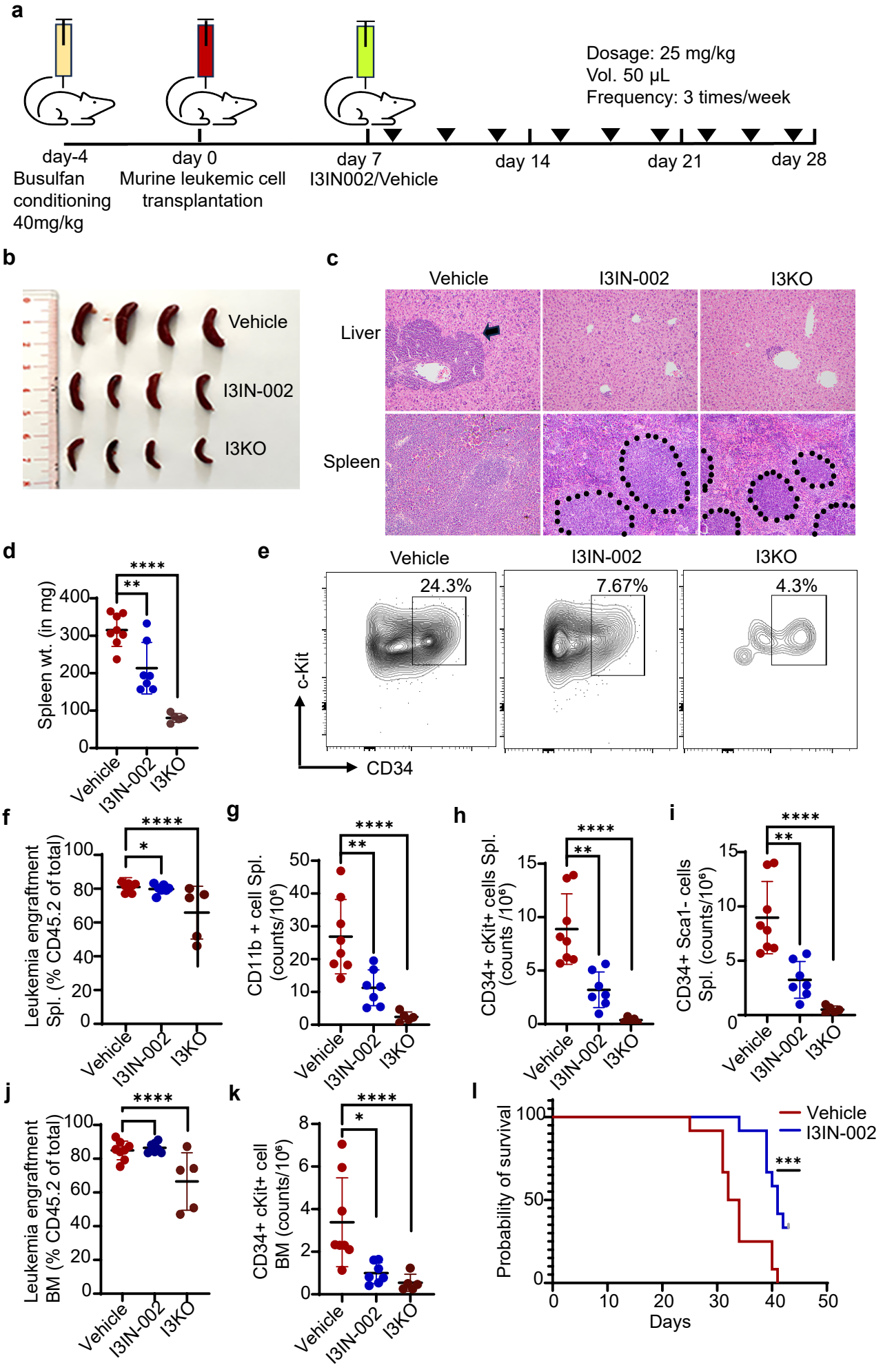
a
Dosage: 25 mg/kg
Vol. 50 µL
Frequency: 3 times/week
day-4
Busulfan conditioning 40mg/kg
day 0
Murine leukemic cell transplantation
day 7
I3IN002/Vehicle
day 14
day 21
day 28
b
Vehicle
I3IN-002
I3KO
c
Vehicle
I3IN-002
I3KO
Liver
Spleen
d
Spleen wt. (in mg)
Vehicle
I3IN-002
I3KO
e
Vehicle
I3IN-002
I3KO
24.3%
7.67%
4.3%
c-Kit
CD34
f
Leukemia engraftment Spl. (% CD45.2 of total)
g
CD11b + cell Spl. (counts/10⁶)
h
CD34+ cKit+ cells Spl. (counts /10⁶)
i
CD34+ Sca1- cells Spl. (counts/10⁶)
j
Leukemia engraftment BM (% CD45.2 of total)
k
CD34+ cKit+ cell BM (counts/10⁶)
l
Probability of survival
Days
Vehicle
I3IN-002

**Figure 5.**

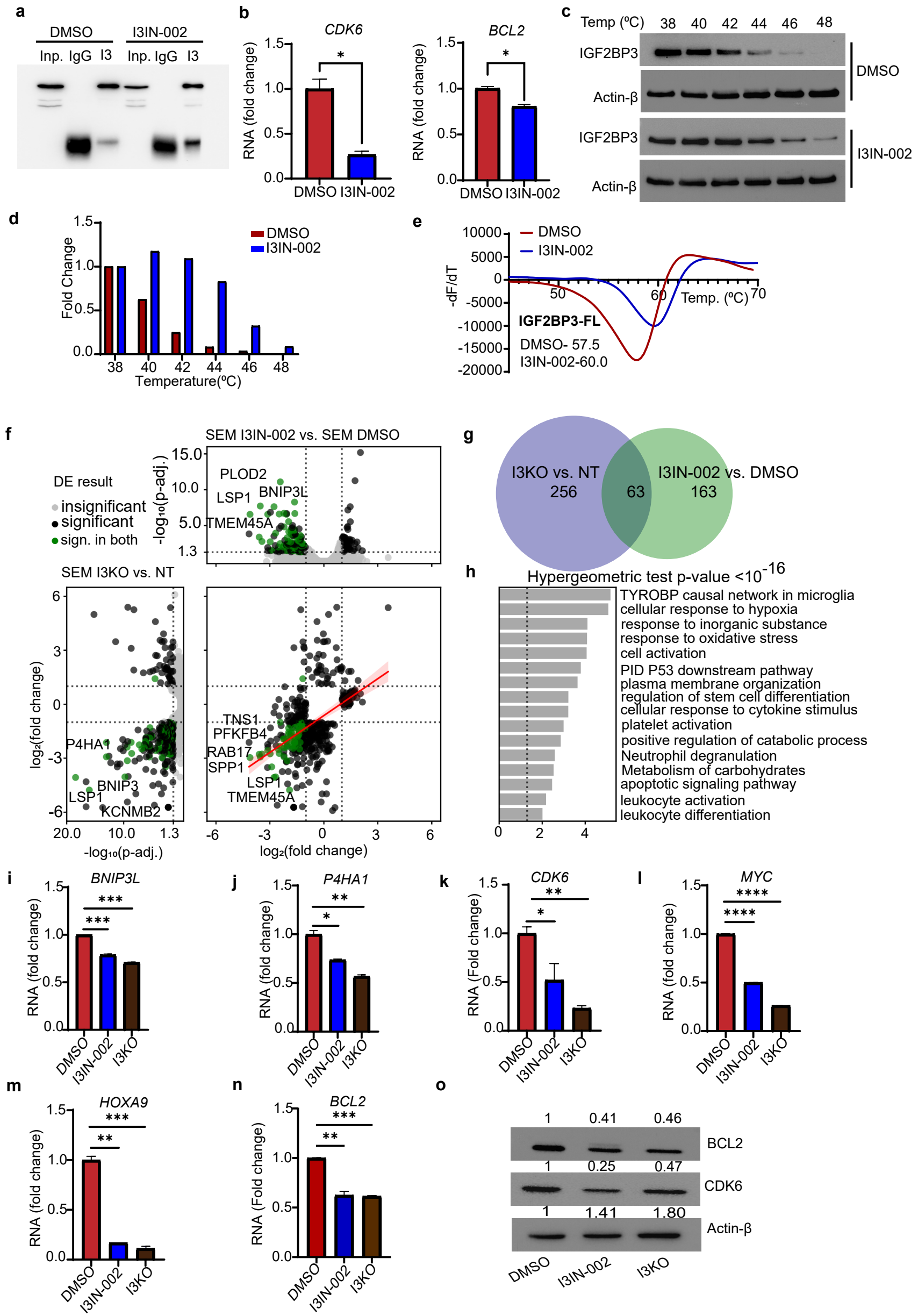
a
DMSO
I3IN-002
Inp. IgG I3 Inp. IgG I3
b
CDK6
BCL2
RNA (fold change)
DMSO I3IN-002
c
Temp (ºC) 38 40 42 44 46 48
IGF2BP3
Actin-β
DMSO
I3IN-002
d
Fold Change
Temperature(ºC)
DMSO
I3IN-002
e
-dF/dT
Temp. (ºC)
IGF2BP3-FL
DMSO- 57.5
I3IN-002-60.0
f
SEM I3IN-002 vs. SEM DMSO
DE result
insignificant
significant
sign. in both
-log10(p-adj.)
PLOD2
LSP1
BNIP3L
TMEM45A
SEM I3KO vs. NT
log2(fold change)
P4HA1
BNIP3
LSP1
KCNMB2
TNS1
PFKFB4
RAB17
SPP1
LSP1
TMEM45A
g
I3KO vs. NT
256
63
I3IN-002 vs. DMSO
163
h
Hypergeometric test p-value <10-16
TYROBP causal network in microglia
cellular response to hypoxia
response to inorganic substance
response to oxidative stress
cell activation
PID P53 downstream pathway
plasma membrane organization
regulation of stem cell differentiation
cellular response to cytokine stimulus
platelet activation
positive regulation of catabolic process
Neutrophil degranulation
Metabolism of carbohydrates
apoptotic signaling pathway
leukocyte activation
leukocyte differentiation
i
BNIP3L
j
P4HA1
k
CDK6
l
MYC
m
HOXA9
n
BCL2
RNA (fold change)
RNA (Fold change)
DMSO I3IN-002 I3KO
o
1 0.41 0.46
BCL2
1 0.25 0.47
CDK6
1 1.41 1.80
Actin-β
DMSO I3IN-002 I3KO